7B.5 RAPID INTENSIFICATION OF A SHEARED, FAST-MOVING HURRICANE OVER THE GULF STREAM

Leon Nguyen* and John Molinari

University at Albany, SUNY

1. INTRODUCTION

Vertical wind shear has been known to have a generally negative influence on tropical cyclone intensity (e.g. Kaplan et al. 2010). However, rapidly intensifying tropical cyclones undergoing moderate to high ambient vertical wind shear and possessing a highly asymmetric convective structure have been documented in the literature (e.g. Molinari and Vollaro 2010). The processes involved in asymmetric rapidly intensifying tropical cyclones have garnered increasing interest in the research community.

This study documents the rapid intensification of Hurricane Irene (1999), which intensified under increasing vertical wind shear and developed a highly asymmetric structure as a result. Also, Irene was rapidly translating and was tracking near the warm Gulf Stream during the RI period. The impact of all of these factors on the asymmetric structure and rapid intensification of Hurricane Irene will be evaluated.

2. DATA SOURCES AND CALCULATIONS

The data sources for this study include (i) U.S. Air Force reconnaissance data; (ii) Weather-Surveillance Radar-1988 (WSR-88D) data; (iii) cloud-to-ground lightning data from the National Lightning Detection Network (NLDN); (iv) 6-hourly gridded analyses (1.125° resolution) from the European Center for Medium-Range Weather Forecasts (ECMWF); (v) sea-surface temperature data from the Advanced High Resolution Radiometer (AVHRR) aboard NOAA polar-orbiting satellites; and (vi) Ambient vertical wind shear estimates from the Statistical Hurricane Intensity Prediction Scheme (SHIPS) database (DeMaria et al. 2005).

Aircraft reconnaissance data included flight-level wind speed and direction, temperature, and D value at the 850 hPa level for all flights relevant to this study. During the RI period, dewpoint measurements after 0231 UTC on the 18th were unavailable because they were unrealistically low (below 10°C) with virtually no spatial variation. The center of Irene was defined using the minimum D value following Molinari and Vollaro (2010).

Level III base reflectivity data from the Wilmington and Morehead City radar sites were available from the lowest (0.5°) elevation angle out to a distance of 230 km. Level II reflectivity and velocity data from multiple elevation angles were available out to a distance of 460 km from Wilmington and Raleigh, but not from Morehead City.

WSR-88D radial velocity data at the 0.5°, 1.5°, and 2.5° elevation angles were used to diagnose vortex tilt following Molinari and Vollaro (2010). The radial velocity data show the component of the wind going away from (outbound) or towards the radar site (inbound). Winds perpendicular to the radar beam have zero radial velocity. This zero isodop denotes the dividing line between outbound winds and inbound winds. The displacement of the zero isodop position with height represents the component of vortex tilt perpendicular to the line segment between the radar site and the TC center.

Base reflectivity data were composited about the storm center over a series of one hour periods. These are intended to show the time evolution of the precipitation structure about the vortex, but with the limitation that individual cells are smoothed out. To construct the azimuthally averaged radar reflectivity Hovmöllers, the data were first translated to storm-relative coordinates. The data were then bilinearly interpolated to cylindrical coordinates, with radial resolution of 1 km and azimuthal resolution of 1°, roughly following Corbosiero et al. (2005).

3. STORM HISTORY AND LARGE-SCALE ENVIRONMENT

Irene underwent a period of rapid intensification (RI) while off the North Carolina coast. The maximum sustained surface winds increased from 65 knots at 1200 UTC 17 October to 95 knots at 0600 UTC 18 October, meeting the 30 kt/24 hour threshold for rapid intensification (Kaplan et al. 2010). From 0106-0757 UTC on the 18th, the pressure fell at a 2.5 hPa/hr rate to a minimum of 958 hPa. Table 1 shows estimates of 6-hourly storm motion and ambient vertical wind shear from SHIPS and ECMWF gridded analysis. During the RI period, Irene accelerated towards the northeast from 9-10 m s^{-1} to near 18 m s^{-1}, and the ambient southwesterly vertical wind shear increased from 6-7 m s^{-1} to10-13 m s^{-1}. During RI both the storm motion and shear vectors were approximately aligned.

4. VORTEX-SCALE EVOLUTION DURING RAPID INTENSIFICATION

a. *Azimuthal wavenumber-1 asymmetry*

Figure 1 shows a sequence of radar reflectivity 1-hour composites from 1914 UTC on the 17th (prior to RI) to 0657 UTC on the 18th (one hour prior to peak intensity). In this discussion, “forward” and “rear” refer

* *Corresponding author address: Leon Nguyen, Dept. of Atmospheric and Environmental Sciences, ES 339B, University at Albany/SUNY, 1400 Washington Ave. Albany, NY 12222; e-mail: lnguyen@albany.edu*

Table 1: Vertical wind shear and storm motion in Hurricane Irene. Shear is calculated between 850 and 200 hPa averaged within 500 km of the center from the SHIPS database (column 2) and ECMWF gridded analyses (column 3). Storm motion uses centered differencing over 6 hours from the aircraft reconnaissance-based track.

Time	SHIPS Vertical Wind Shear	ECMWF Vertical Wind Shear	6-hourly storm motion
1200 UTC 17 Oct.	233° at 5.1 m s^{-1}	245° at 6.5 m s^{-1}	187° at 5.1 m s^{-1}
1800 UTC 17 Oct.	211° at 7.7 m s^{-1}	236° at 5.7 m s^{-1}	228° at 8.3 m s^{-1}
0000 UTC 18 Oct.	224° at 5.8 m s^{-1}	238° at 7.3 m s^{-1}	233° at 10.0 m s^{-1}
0600 UTC 18 Oct.	233° at 13.1 m s^{-1}	242° at 10.4 m s^{-1}	232° at 15.5 m s^{-1}
1200 UTC 18 Oct.	237° at 14.8 m s^{-1}	238° at 11.4 m s^{-1}	237° at 20.2 m s^{-1}

to the location with respect to storm motion. Prior to RI (Fig. 1a), reflectivity maxima were present outside the 50 km radius both downshear-right (right-forward) and upshear (rear) of the center. Over the next two hours (Fig. 1b) several intensifying inner rain bands, comprised of embedded convective cells, spiraled cyclonically inwards around the north side (downshear-left and left-forward) of the center. These bands continued to wrap around the western and southern sides, and by 0000 UTC on the 18th (Fig. 1c), the reflectivity structure around the center became more symmetric.

The rather symmetric precipitation structure in the inner core was short-lived, however. The ambient vertical wind shear and storm motion, both pointing to the northeast, increased substantially after 0000 UTC on the 18th (Table 1). As a result, the reflectivity structure became more asymmetric during RI, not only in the inner core but also in the inner and outer band regions. Figure 1d shows a reflectivity minimum resembling an eye with composite reflectivity exceeding 35 dBz located downshear (forward) between 0134-0234 UTC on the 18th. The azimuthal wavenumber-1 asymmetry increased further over the next 4 hours (Fig. 1e-f), with the high reflectivity downshear to downshear-right (forward to right-forward) forming a crescent-shaped band in the composite just 5-15 km from the center, while the upshear (rear) half became nearly devoid of precipitation.

b. *Evidence of vortex tilt*

Figure 2 shows storm-relative zero isodop positions at three elevation angles from the Wilmington, NC radar. Near 0000 UTC on the 18th (Fig. 2a), there appeared to be a substantial northeastward shift in the zero isodop with height outside of the 20 km radius (outer vortex), indicative of a northeastward tilt of the vortex with height. The outer vortex tilt was about 79° from the vertical axis. This tilt was consistent with an azimuthal

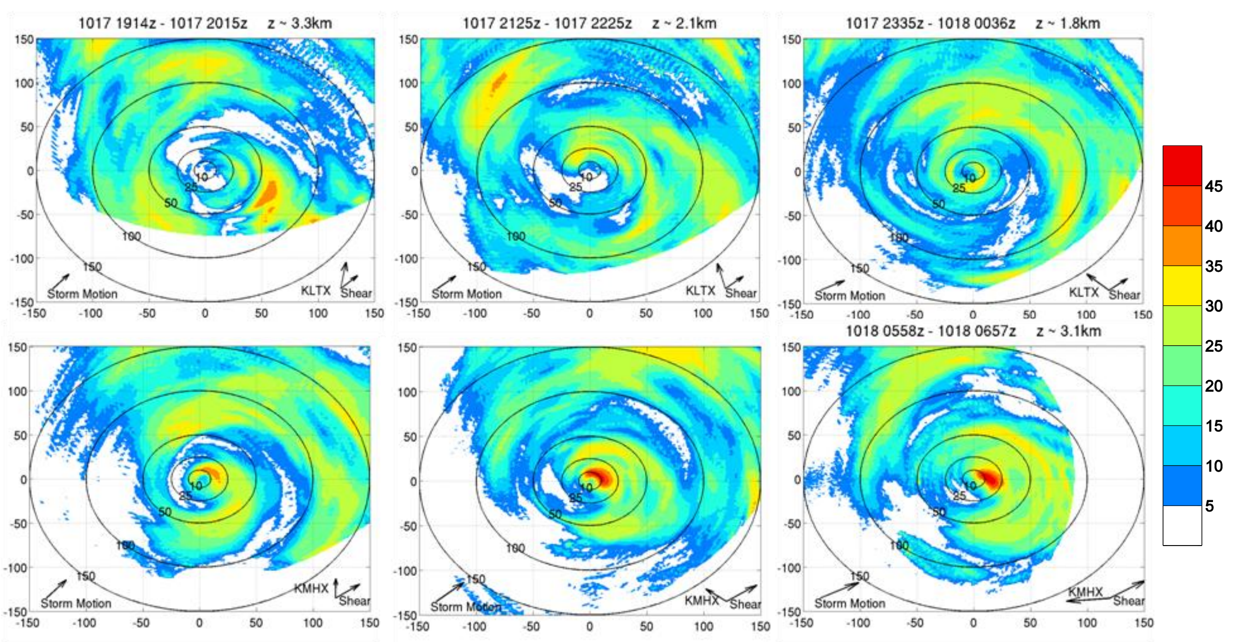

Fig. 1: WSR-88D radar reflectivity (dBz) for the 0.5° elevation angle, composited about the storm center during the time ranges specified. (a), (b), and (c) are from the Wilmington, NC radar; (d), (e), and (f) are from the Morehead City, NC radar. Range rings represent distances of 10, 25, 50, 100, and 150 km from the tropical cyclone center. Average radar beam heights at the TC center during the composited time periods are given in the upper right.

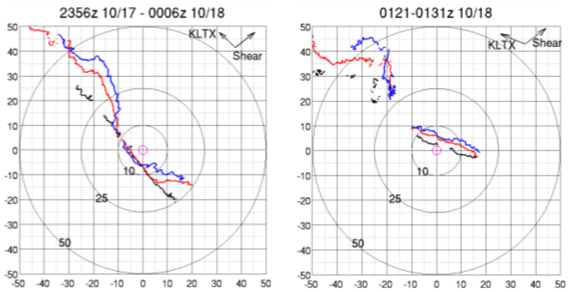

Fig. 2: Plot of the zero-isodop position relative to the storm center at the 0.5° (black), 1.5° (red), and 2.5° (blue) elevation angles derived from the radial velocity data. The average height of the radar beam over the center in (a) is approximately 1.8 km (0.5° tilt), 3.7 km (1.5° tilt), and 5.5 km (2.5° tilt); and in (b) is approximately 2.3 km (0.5° tilt), 4.8 km (1.5° tilt), and 7.1 km (2.5° tilt).

wavenumber-1 asymmetry in reflectivity outside the core (Fig. 1c). In contrast, there appeared to be very little shift in the zero isodop with height of the vortex within the 20 km radius (inner vortex), consistent with the relatively symmetric inner core reflectivity structure (Fig. 1c). An hour and a half later (Fig. 2b), some inner-vortex tilt towards the north-northeast with height was diagnosed, consistent with an increasing wavenumber-1 reflectivity asymmetry in the inner core (Fig. 1d). The inner-vortex tilt was about 53° from the vertical axis. After this time, the center moved too far away from the radar site to evaluate vortex tilt.

c. *Azimuthally averaged reflectivity*

Radius-time Hovmöllers of azimuthally averaged radar reflectivity and mean storm-relative tangential wind are shown in Figure 3. Prior to 2100 UTC on the 17th (Fig. 3a), the azimuthally averaged reflectivity was weak (< 15 dBz) within 40 km of the center. Reflectivity slowly increased within the 40 km radius during the 2000-2300 UTC 17 Oct. time period. Shortly after 2300 UTC on the 17th, a >27.5 dBz azimuthally averaged reflectivity maximum developed 10-20 km from the center, well within the 50 km radius of maximum winds. This maximum coincided with the development of a closed eye seen in Figure 1c and marked the beginning of an accelerated decrease in minimum central pressure. After 0100 UTC on the 18th, the azimuthally averaged reflectivity from the Morehead City radar experienced a dramatic increase inside the radius of maximum winds (Fig. 3b). The azimuthally averaged reflectivity began to exceed 30 dBz within 10 km at around 0300 UTC on the 18th and reached a maximum of nearly 40 dBz at 4-8 km from the center at 0500 UTC on the 18th. The high reflectivities at the center in Fig. 3 are likely an artifact of the offset center position. This increase in azimuthally averaged reflectivity was also observed from the Wilmington radar (Fig. 3a) despite the increasing distance from that radar, indicating that the increase of reflectivity was due to heavier

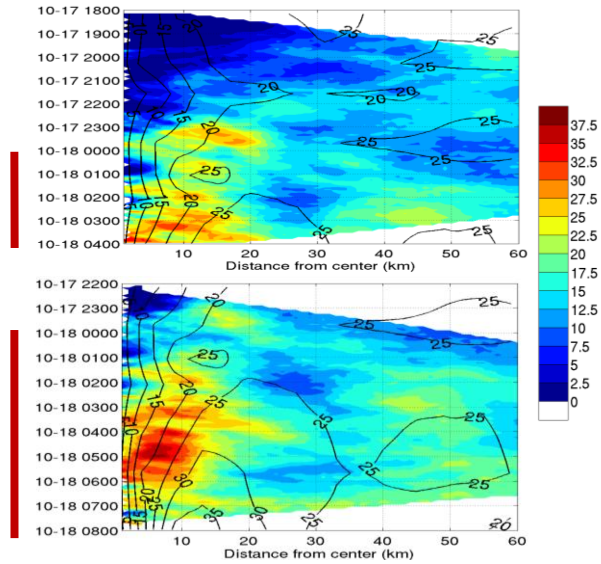

Fig. 3: Radius-time Hovmöller of azimuthally averaged radar reflectivity from a) the Wilmingon, NC radar, and b) the Morehead City, NC radar. Mean storm-relative tangential wind (m s^{-1}) is shown in black contours. Dark red bar on the left denotes the RI period.

precipitation and not due to closer proximity to the radar. The azimuthally averaged reflectivity then decreased some after 0600 UTC on the 18th, although that may be partially attributed to the distance between the center and the radar site (> 160 km). Between 0300-0700 UTC on the 18th, the reflectivity structure around the center of Irene was very asymmetric due to the increasing shear and storm motion (Fig. 1e-f), but the strong reflectivities to the northeast of the center more than offset the weak reflectivities to the southwest, resulting in a large increase in the azimuthal average of reflectivity. Importantly, the high azimuthally averaged reflectivity occurred almost entirely within the radius of maximum winds (RMW) (Fig. 3b), which was contracting from around 50 km at 0000 UTC to around 10 km by 0800 UTC on the 18th.

5. DISCUSSION

The development of intense convection near the center contributed significantly to the rapid intensification of Irene. Assuming that radar reflectivity can be used as an indicator of diabatic heating, the increase in azimuthally averaged heating within 5-10 km of the center (Fig. 3b) occurred inside the RMW, which was contracting from about 22 to 13 km during the period (Fig. 3). Diabatic heating within the RMW has been found to be most effective for producing intensification (Nolan et al. 2007; Vigh and Schubert 2009). In addition, intensification efficiency increases with decreasing RMW following the arguments of Pendergrass and Willoughby (2009).

Although the magnitude of the wavenumber-1 convective asymmetry was increasing during rapid

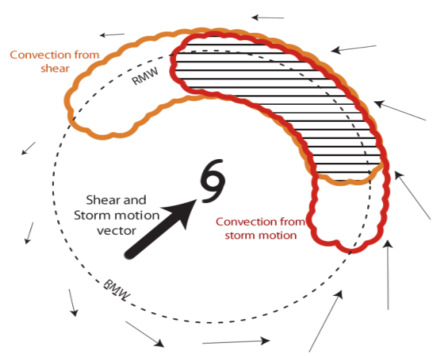

Fig. 4: Schematic diagram summarizing the interaction between the strong vertical wind shear and fast storm motion during the RI period. Convective areas favored by shear and storm motion following Corbosiero and Molinari (2003) are shown by the orange and red regions, respectively. The straight arrows represent the earth-relative surface winds.

intensification (Fig. 1c-f), the intense reflectivity to the northeast of the center more than offset the weak values to the southwest, resulting in the considerable increase in the azimuthal average shown in Fig. 3. The storm responded more to the azimuthal average of diabatic heating than to the degree of symmetry in diabatic heating, which is consistent with the results of Nolan et al. (2007).

Figure 4 shows a schematic diagram of the hypothesized influences on the rapid intensification of Hurricane Irene. Only the vicinity of the radius of maximum winds is shown. As the shear increased after 0000 UTC on the 18th (Table 1), convective cells would be expected to initiate downshear-right and intensify as they move into the downshear quadrant (e.g., Heymsfield et al. 2001). The rapidly accelerating storm motion from 9-10 m s^{-1} to 18 m s^{-1} during the RI period (Table 1) ensures a clear signal in storm motion-induced asymmetries. As a result, the favored regions for upward motion based on previous work on vertical wind shear and storm motion overlapped in the northeast quadrant, exactly where the strongest convection developed (Fig. 1d-f).

The majority of storms experiencing ambient vertical wind shear above 10 m s^{-1} do not intensify. One possible reason for this was provided by Riemer et al. (2010). The tilt of the outer vortex in a sheared storm induces an azimuthal wavenumber-1 asymmetry in convection outside the inner core, resulting in downward fluxes of low θ_e air into the inflow layer. Surface fluxes are insufficient to restore moist enthalpy as this air reaches the eyewall region, reducing the azimuthal-mean θ_e and weakening the storm (Tang and Emanuel 2010). In Hurricane Irene, a tilt of the outer vortex was observed (Fig. 2) as well as a corresponding region of convection downshear to downshear-right outside the core and over the Gulf Stream (not shown), but the storm did not weaken. We speculate that large surface enthalpy fluxes from the Gulf Stream in this part of the storm might have helped offset the negative influence of the downdrafts in the outer convective region.

Although the azimuthal distribution of the convection during the RI is well explained by the effects of ambient vertical wind shear and fast storm motion, why the convection occurred so close to the center in the first place under a strong ambient vertical wind shear regime remains an unanswered question.

References

Corbosiero, K. L., and J. Molinari, 2003: The relationship between storm motion, vertical wind shear, and convective asymmetries in tropical cyclones. *J. Atmos. Sci.*, 60, 366–376.

Corbosiero, K. L., J. Molinari, and M. L. Black, 2005: The structure and evolution of Hurricane Elena (1985). Part I: Symmetric intensification. *Mon. Wea. Rev.*, 133, 2905–2921.

DeMaria, M., M. Mainelli, L. K. Shay, J. A. Knaff, and J. Kaplan, 2005: Further improvements to the Statistical Hurricane Intensity Prediction Scheme (SHIPS). *Wea. Forecasting*, 20, 531–543.

Heymsfield, G. M., J. B. Halverson, J. Simpson, L. Tian, and T. P. Bui, 2001: ER-2 doppler radar investigations of the eyewall of Hurricane Bonnie during the Convection and Moisture Experiment-3. *J. Appl. Meteor.*, 40, 1310–1330.

Kaplan, J., M. DeMaria, and J. A. Knaff, 2010: A revised tropical cyclone rapid intensification index for the Atlantic and Eastern North Pacific basins. *Wea. Forecasting*, 25, 220–241.

Molinari, J., and D. Vollaro, 2010: Rapid intensification of a sheared tropical storm. *Mon. Wea. Rev.*, 138, 3869–3885.

Nolan, D. S., Y. Moon, and D. P. Stern, 2007: Tropical cyclone intensification from asymmetric convection: Energetics and efficiency. *J. Atmos. Sci.*, 64, 3377–3405.

Pendergrass, A. G., and H. E. Willoughby, 2009: Diabatically induced secondary flows in tropical cyclones. Part I: Quasisteady forcing. Mon. Wea. Rev., 137, 805–821.

Riemer, M., M. T. Montgomery, and M. E. Nicholls, 2010: A new paradigm for intensity modification of tropical cyclones: Thermodynamics impact of vertical wind shear on the inflow layer. *Atmos. Chem. Phys.*, 10, 3163–3188.

Tang, B., and K. Emanuel, 2010: Midlevel ventilation's constraint on Tropical Cyclone intensity. *J. Atmos. Sci.*, 67, 1817–1830.

Vigh, J. L., and W. H. Schubert, 2009: Rapid development of the tropical cyclone warm core. *J. Atmos. Sci.*, 66, 3335–3350.